



Yb sensitising of Er^{3+} up-conversion emission in $\text{KGd}(\text{WO}_4)_2:\text{Er}:\text{Yb}$ single crystals

M. Rico^{a,*}, M.C. Pujol^b, X. Mateos^b, J. Massons^b, C. Zaldo^a, M. Aguiló^b, F. Díaz^b

^aInstituto de Ciencia de Materiales de Madrid, Consejo Superior de Investigaciones Científicas, 28049 Madrid, Spain

^bLaboratori de Física Aplicada i Cristal·lografia, Universitat Rovira i Virgili, 43005 Tarragona, Spain

Abstract

$\text{KGd}_{(1-x-y)}\text{Er}_x\text{Yb}_y(\text{WO}_4)_2$ ($x/y=0.024/0$, $0.02/0.022$ and $0.019/0.066$) single crystals have been grown by the top seeded solution growth slow cooling method using $\text{K}_2\text{W}_2\text{O}_7$ as solvent. Erbium concentration was selected at $[\text{Er}]=1.2\text{--}1.5\times 10^{20}\text{ cm}^{-3}$ in order to minimise Er–Er non-radiative losses and the ytterbium concentration was varied in the range $[\text{Yb}]=0\text{--}4.2\times 10^{20}\text{ cm}^{-3}$. The optical absorption in the 850–1100 nm spectral range is characterised by the overlap between ytterbium $^2\text{F}_{5/2}$ and erbium $^4\text{I}_{11/2}$ manifolds. At room temperature the green $^4\text{S}_{3/2}\text{Er}^{3+}$ emission has been excited by energy transfer from the $^2\text{F}_{5/2}$ (934.2, 953.2 and 980.8 nm) ytterbium multiplet. The up-converted emission is weakly polarised and within the concentration range studied its intensity increases with the Yb^{3+} concentration. © 2001 Elsevier Science B.V. All rights reserved.

Keywords: Optical properties; Luminescence; Non-linear optics

1. Introduction

Up-conversion in trivalent rare earths is intensively studied in order to produce visible solid state lasers pumped by infrared laser diodes. The search is at present focused on the optimisation of the process including the search for laser hosts with large rare earth absorption and emission cross-sections as well as low non-radiative losses.

$\text{KGd}(\text{WO}_4)_2$ (hereafter KGW) is a novel single crystal laser which is receiving a lot of attention due to the high efficiency of the 1.06 μm Nd^{3+} laser emission [1] and by the coupling of this emission with optical phonons of the lattice giving rise to self-induced frequency shifting [2,3].

Er^{3+} is maybe the most studied rare earth ion for up-conversion processes due to its efficient green ($^4\text{S}_{3/2}\rightarrow^4\text{I}_{15/2}$) photoluminescence, which can be excited by diode lasers in the 990–970 nm ($^4\text{I}_{15/2}\rightarrow^4\text{I}_{11/2}$) and 805–795 nm ($^4\text{I}_{15/2}\rightarrow^4\text{I}_{9/2}$) spectral regions. In fact, laser emission excited by up-conversion has been demonstrated at room temperature in several crystals, namely YLiF_4 [4–6], $\text{Y}_3\text{Al}_5\text{O}_{12}$ [5,6], and $\text{Lu}_3\text{Al}_5\text{O}_{12}$ [6]. The main limitation of Er^{3+} for up-conversion is the weak ground

state absorption of the $^4\text{I}_{11/2}$ and $^4\text{I}_{9/2}$ multiplets, while on the other hand the increase of the Er^{3+} concentration beyond a certain limit leads to higher non-radiative losses. In KGW it was found that the maximum up-conversion efficiency is achieved around $1\text{--}2\times 10^{20}$ erbium atoms/ cm^3 [7]. In order to improve the overall up-conversion efficiency Yb^{3+} may be used as a sensitizer of the $^4\text{I}_{11/2}$ Er^{3+} multiplet [8,9].

The Yb^{3+} [10,11] and Er^{3+} [7,12] spectroscopy in KGW have been described separately. In this work, we present an investigation of the cooperative up-conversion processes in KGW single crystal doped with Yb and Er.

2. Crystal growth

$\text{KGd}_{(1-x-y)}\text{Er}_x\text{Yb}_y(\text{WO}_4)_2$ (hereafter KGW:Er:Yb) single crystals have been grown by the top seeded solution growth (TSSG) slow cooling method using $\text{K}_2\text{W}_2\text{O}_7$ as solvent. A detailed description of the growth equipment and procedures can be found in previous works [13,14]. The solution compositions in the crystal growth experiments were 88.5% $\text{K}_2\text{W}_2\text{O}_7$ (solvent) and 11.5% $\text{KGd}_{(1-x-y)}\text{Er}_x\text{Yb}_y(\text{WO}_4)_2$ (solute) molar ratio. Table 1 summarises the growth details of the samples used.

The molar erbium and ytterbium concentrations in the

*Corresponding author.

E-mail address: mauricio@icmm.csic.es (M. Rico).

Table 1
Details about crystal growth experiments

A ^a	B ^b	C ^c	D ^d	E ^e	F ^f	G ^g	H ^h	I ⁱ	J ^j	K ^k	L ^l	M ^m	N ⁿ
3%Er	b	0.1 0.05	2.2 8.5	Free	14.5	12	4.8	0.024	–	0.82	–	1.5	–
2.5%Er 2.5%Yb	b	0.1 0.05	1 10	Few	8.5	10.5	3	0.020	0.022	0.87	0.79	1.2	1.4
2.5%Er 7.5%Yb	b	0.1 0.05	2 8	Free	14	10	5	0.019	0.066	0.88	0.74	1.2	4.2

^a A: RE₂O₃/(Gd₂O₃ + RE₂O₃) ratio in the solution, at%.

^b B: seed orientation.

^c C: cooling rate, °C/h.

^d D: cooling interval, °C.

^e E: macrodefects.

^f F: crystal dimensions along **c** direction, mm.

^g G: crystal dimensions along **a*** direction, mm.

^h H: crystal dimensions along **b** direction, mm.

ⁱ I: *x* in the crystal [KGd_{1-x-y}Er_xYb_y(WO₄)₂].

^j J: *y* in the crystal [KGd_{1-x-y}Er_xYb_y(WO₄)₂].

^k K: distribution coefficient, $K_{Er^{3+}} = \frac{(molEr^{3+}/(molGd^{3+} + molEr^{3+} + molYb^{3+}))_{crystal}}{(molEr^{3+}/(molGd^{3+} + molEr^{3+} + molYb^{3+}))_{solution}}$.

^l L: distribution coefficient, $K_{Yb^{3+}} = \frac{(molYb^{3+}/(molGd^{3+} + molYb^{3+} + molEr^{3+}))_{crystal}}{(molYb^{3+}/(molGd^{3+} + molYb^{3+} + molEr^{3+}))_{solution}}$.

^m M: [Er³⁺] (×10²⁰ cm⁻³).

ⁿ N: [Yb³⁺] (×10²⁰ cm⁻³).

crystal, [Er] and [Yb], respectively, were determined by electron probe microanalysis (EPMA), using CAMECA Camebax SX 50 equipment.

KGW crystal is monoclinic, with *C2/c* space group [12]. Er³⁺ and Yb³⁺ are located in the C₂ site replacing Gd³⁺, and the twofold principal axis of the defect is parallel to the crystallographic **b** axis. The principal axes of the indicatrix are labelled *m*, *g* and *p*. The smallest refractive index *p* is parallel to crystallographic **b** axis. The two other principal axes, *m* and *g*, lie in the crystallographic **ac** plane. The *g* axis forms an angle with the crystallographic **c** axis of 21.5° in the clockwise direction when looking from the positive end of the **b** axis. The *m* axis is orthogonal to the *g* axis.

3. Optical spectroscopy

The polarised optical absorption spectra were recorded using a Varian spectrophotometer, model 5E. The spectrophotometer beam was polarised with a Glan-Taylor polariser and the polarisation configuration is selected by changing the sample orientation.

Up-conversion emission was excited with a continuous wave Ti-sapphire laser. The excitation wavelength was calibrated with an optical multichannel analyser OTSUKA 1100, within ±0.2 nm and the excitation spectra have been corrected by the spectral emission response of the Ti-sapphire laser. The emission was analysed using a Spex 500 M spectrometer (*f*=50 cm) and the signal was detected with a photomultiplier and a lock-in.

Fig. 1a shows the room temperature ground state optical absorption (GSA), α_{GSA}, of KGW:Er:Yb crystals in the 880–1060 nm range for increasing Yb concentration. These spectra consist of overlapped bands corresponding to the ⁴I_{15/2}→⁴I_{11/2} Er³⁺ and ²F_{7/2}→²F_{5/2} Yb³⁺ transitions.

Fig. 1b shows the optical absorption changes for light polarised along the principal axes of the indicatrix. The three spectra present the same peaks, although the relative intensities of the peaks depend on the polarisation configuration. Er³⁺ and Yb³⁺ have semi integer total angular momentum, *J*, therefore polarisation selection rules are not expected due to the C₂ symmetry group. The absorption changes observed should be related to the material birefringence and to changes in the corresponding transition moment integrals. Table 2 summarises the ground state absorption cross-sections (σ_{GSA}=α_{GSA}/*N*, *N* being the atom concentration) of Er³⁺ and Yb³⁺ for relevant wavelengths in this range. The Yb σ_{GSA} values calculated in this work are smaller than those reported previously [10]. In our view, this difference is due to a previous overestimation of the Yb absorption coefficient (compare the α(981 nm)=40 cm⁻¹ value used in [10] with Fig. 1 of this reference and our Fig. 1a). It is worth remarking that Yb³⁺ generally achieves higher σ_{GSA} values than Er³⁺.

Fig. 2 shows the emission and excitation spectra of the Er³⁺ up-conversion in KGd(WO₄)₂ pumping Yb. The two complex green emissions observed are due to radiative transitions of Er³⁺ from the ²H_{11/2} and ⁴S_{3/2} multiplets to the ground ⁴I_{15/2} multiplet. The presence of Yb³⁺–Er³⁺ energy transfer is therefore evident. Fig. 3 shows a

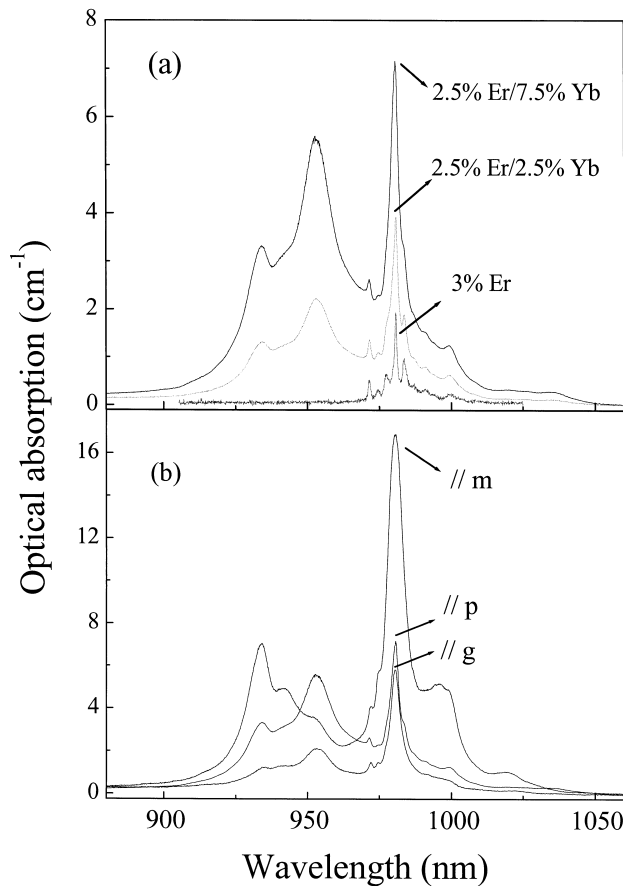


Fig. 1. (a) Room temperature p-polarised ground state optical absorption for increasing Yb concentration in $\text{KGd}(\text{WO}_4)_2:2.5\%\text{Er}:\text{Yb}$ crystals. (b) Room temperature polarised ground state optical absorption of $\text{KGd}(\text{WO}_4)_2:2.5\%\text{Er}:7.5\%\text{Yb}$ single crystals.

Table 2

Room temperature ground state absorption cross-sections, σ_{GSA} , for the relevant wavelengths of Er^{3+} and Yb^{3+} in KGW^a

	λ (nm)	σ_{GSA} (10^{-21} cm^2)		
		//g	//m	//p
Yb^{3+}	934.25	2.6	16.8	8.1
${}^2\text{F}_{7/2} \rightarrow {}^2\text{F}_{5/2}$	942	2.8	11.7	7.5
	953.15	4.9	8.2	13.3
	980.8	13.8	39.8	14.9
	995.8	1.5	11.9	2.6
	999.7	1.3	10.8	2.7
	1019.5	–	2.4	–
	1022.3	0.4	–	–
	1036	–	–	0.07
Er^{3+}	978.2	–	5.7–13	–
${}^4\text{I}_{15/2} \rightarrow {}^4\text{I}_{11/2}$	981	–	–	5–10
${}^4\text{I}_{15/2} \rightarrow {}^4\text{S}_{3/2}$	543.9	–	–	4–8

^a The uncertainty for erbium arises from the different concentrations obtained by EPMA and PIXE measurements.

schematic energy diagram of the process. The shape of the emission is slightly sensitive to the polarisation conditions of the analysed light: the two most intense maxima are observed at $\lambda_{\text{EMI}} = 553.8$ and 555.6 nm. The excitation spectra generally resemble the ground state absorption spectra (Fig. 1b), although the most intense peak in //m configuration (at 980 nm) is likely depleted due to the strong auto-absorption of the excitation beam.

Fig. 4 compares the up-conversion emission intensity of crystals with a nearly constant Er concentration ($[\text{Er}] \approx 1.2\text{--}1.5 \times 10^{20} \text{ cm}^{-3}$) and increasing Yb concentrations ($[\text{Yb}] = 0, 1.4 \times 10^{20}$ and $4.1 \times 10^{20} \text{ cm}^{-3}$). In all samples the Er concentration is in the range of maximum up-conversion emission intensity found in single doped $\text{KGW}:\text{Er}$ [7]. Exciting at 953 nm, the ${}^4\text{S}_{3/2}$ level of erbium is populated exclusively by energy transfer from Yb^{3+} , while exciting at 981 nm simultaneous excitation of Er^{3+} and Yb^{3+} takes place.

4. Discussion

A first step in the development of laser media is to achieve a material with high optical quality. As regards this, the total Gd substitution achieved in the present work was 8.5% in the crystal, implying a total concentration of foreign ions $\sim 5.3 \times 10^{20} \text{ atoms/cm}^3$. Despite of this high degree of substitution, the crystals obtained were free of macrodefects. This good crystal quality is likely related to the high solubility of $\text{KGd}(\text{WO}_4)_2$ in $\text{KEr}(\text{WO}_4)_2$ or $\text{KYb}(\text{WO}_4)_2$ phases. In fact, the two latter phases are isostructural to KGW [15] and the $\text{KGW}\text{--}\text{KErW}$ mixture has a wide solid solution region up to 35 mol% of the Er phase [16].

In addition to the high rare earth admittance of KGW , rare earth ions in this crystal have large ground state absorption cross-sections. In particular those given in Table 2 for Yb and Er are much larger than the maximum ones obtained in the reference material YLiF_4 where up-conversion lasing was achieved [11], namely, $\sigma_{\text{GSA}}({}^2\text{F}_{7/2} \rightarrow {}^2\text{F}_{5/2}) = 8.5 \times 10^{-21} \text{ cm}^2$ for Yb and $\sigma_{\text{GSA}}({}^4\text{I}_{15/2} \rightarrow {}^4\text{I}_{11/2}) = 2.5 \times 10^{-21} \text{ cm}^2$ or $\sigma_{\text{GSA}}({}^4\text{I}_{15/2} \rightarrow {}^4\text{S}_{3/2}) = 1.5 \times 10^{-21} \text{ cm}^2$ for Er. According to the reciprocity principle [17] this indicates an efficient erbium emission if non-radiative losses were minimised.

The good overlap of the GSA between Er and Yb ions at 981 nm (Fig. 1a) eases an efficient energy transfer. This energy transfer can be also observed exciting at higher energy inside the ${}^2\text{F}_{5/2}$ Yb multiplet (930–960 nm) because of the electron thermalisation. In the latter case, Fig. 4 suggests that the Yb–Er energy transfer only takes place for a minimum Yb concentration, i.e. for Yb–Er distances lower than a critical one. This critical distance can be estimated assuming a threshold ytterbium concentration $[\text{Yb}]_{\text{th}} \approx 0.6 \times 10^{20} \text{ cm}^{-3}$ and a continuous dis-

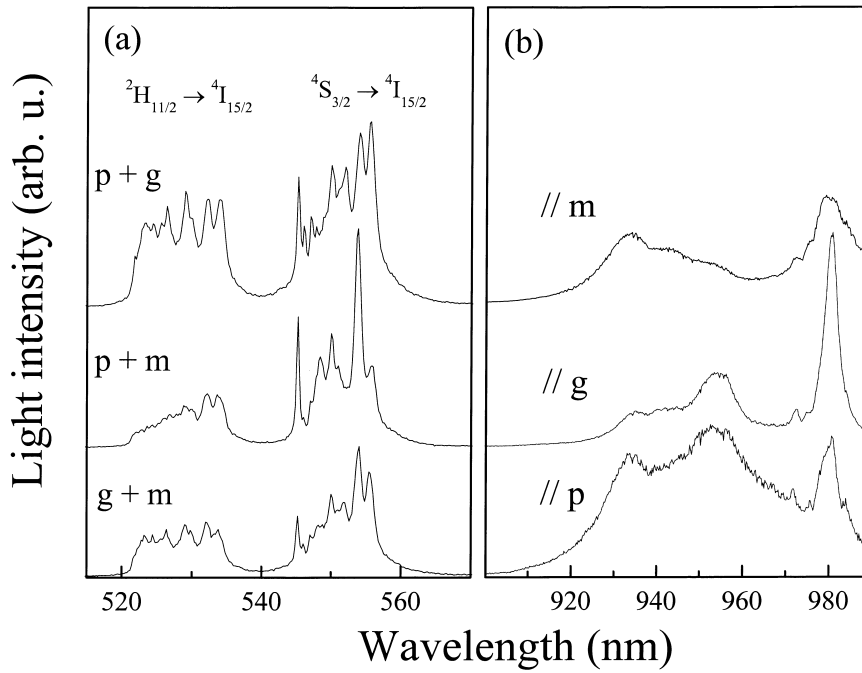


Fig. 2. The 300 K emission and excitation spectra of the erbium up-conversion in $\text{KGd}(\text{WO}_4)_2:2.5\% \text{Er}:7.5\% \text{Yb}$ single crystals. (a) Emission spectra excited with light polarised parallel to the principal m axis at $\lambda_{\text{exc}}=934.2 \text{ nm}$ or p and g axes at $\lambda_{\text{exc}}=953.1 \text{ nm}$. (b) Excitation spectra of the up-conversion, $\lambda_{\text{EMI}}=553.8 \text{ nm}$.

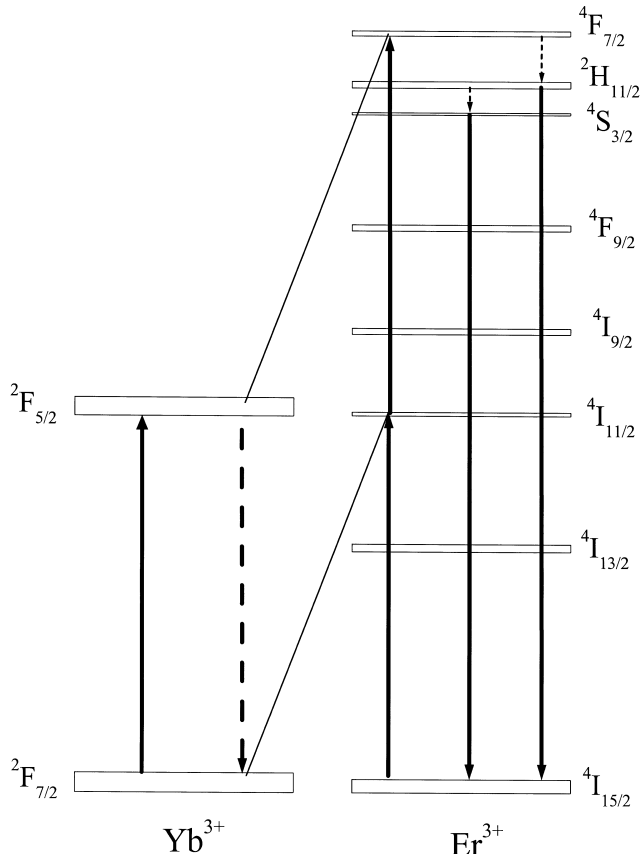


Fig. 3. Schematic energy level diagram of the Er^{3+} and Yb^{3+} multiplets involved in the up-conversion processes in $\text{KGd}(\text{WO}_4)_2:\text{Er}:\text{Yb}$ crystals. Continuous and dashed downward arrows indicate radiative and non-radiative transitions, respectively.

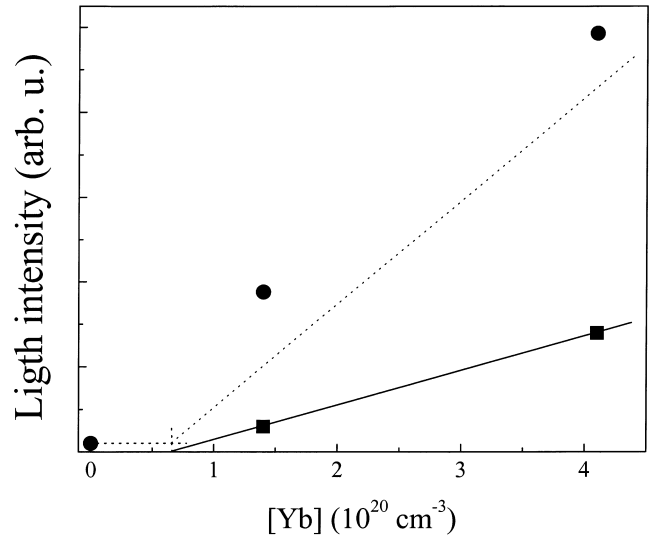


Fig. 4. Evolution of the 300 K Er^{3+} up-conversion intensity with Yb concentration. ■, excitation of the Yb^{3+} ion at $\lambda_{\text{exc}}=953.1 \text{ nm}$ with //p polarised light. ●, simultaneous excitation of the Er^{3+} and Yb^{3+} ions at $\lambda_{\text{exc}}=981 \text{ nm}$ with //m polarised light.

tribution of the impurities, as $R=(4\pi[\text{Yb}]_{\text{th}}/3)^{-1/3} \approx 1.6 \text{ nm}$.

The use of $\lambda_{\text{exc}}=981 \text{ nm}$ produces simultaneous excitation of Er^{3+} and Yb^{3+} ions. As a first approximation, it can be assumed that Er contribution to up-conversion remains constant for all tested samples and this is the only contribution for samples with Yb concentration below $[\text{Yb}]_{\text{th}}$. The dashed line shows the up-conversion intensity

grow regime that could be expected from the change of the Yb absorption from $\lambda=953.1$ nm ($\sigma_{\text{GSA}}//p=13.3\times 10^{-21}$ cm²) to $\lambda=981$ nm ($\sigma_{\text{GSA}}//m=39.8\times 10^{-21}$ cm²). Within the experimental uncertainty the results obtained are close and above the expected regime. This shows that the comparative measurements made for different Yb concentrations are not significantly affected by the possible intensity depletion of the exciting beam, and therefore they are representative of the enhancement of the up-conversion emission intensity with the increase of Yb concentration.

5. Conclusions

Yb and Er codoped KGd(WO₄)₂ single crystals can be achieved by the TSSG-slow cooling method with high Gd–Yb or –Er substitution degree, namely 8.5 mol% of total substitution. Despite this high substitution degree the optical quality of the crystals is very good. Room temperature $^4S_{3/2}\rightarrow^4I_{15/2}$ and $^2H_{11/2}\rightarrow^4I_{15/2}$ Er³⁺ up-conversion emissions in KGW were achieved by energy transfer from the $^2F_{5/2}$ multiplet of Yb³⁺. The optimum erbium concentration for up-conversion is about [Er]=1–2×10²⁰ atoms/cm³, while an increase of the emission intensity with increasing ytterbium concentration is observed under excitation in the optimum conditions, namely, with 981-nm light polarised parallel to the m principal axis of the KGW crystal.

Acknowledgements

This work has been supported by CICYT under projects 2FD97-0912 and MAT99-1077.

References

- [1] A.A. Demidovich, A.P. Shkadarevich, M.B. Danailov, P. Apai, T. Gasmı, V.P. Gribkovskii, A.N. Kuzmin, G.I. Ryabtsev, L.E. Batay, *Appl. Phys. B* 67 (1998) 11.
- [2] A.A. Kaminskii, H. Nishioka, Y. Kubota, K. Ueda, H. Takuma, S.N. Bagayev, A.A. Pavlyuk, *Phys. Status Solidi (a)* 148 (1995) 619.
- [3] A.A. Kaminskii, K. Ueda, H.E. Eichler, J. Findeisen, S. Bagayev, F.A. Kuznetsov, A.A. Pavlyuk, G. Boulon, F. Bourgeois, *Jpn. J. Appl. Phys.* 37 (1995) L1461.
- [4] F. Heine, E. Heumann, T. Danger, T. Schweizer, G. Huber, B. Chai, *Appl. Phys. Lett.* 65 (1994) 383.
- [5] R. Brede, E. Heumann, J. Koetke, T. Danger, H. Huber, B. Chai, *Appl. Phys. Lett.* 63 (1993) 2030.
- [6] T. Danger, J. Koetke, R. Brede, E. Heumann, G. Huber, B.H.T. Chai, *J. Appl. Phys.* 1413 (1994) 76.
- [7] M. Rico, M.C. Pujol, F. Díaz, C. Zaldo, *Appl. Phys. B* 72 (2001) 157.
- [8] P.E.A. Möbert, E. Heumann, G. Huber, B.H.T. Chai, *Opt. Lett.* 22 (1997) 1412.
- [9] R.H. Page, K.I. Schaffers, P.A. Waide, J.B. Tassano, S.A. Payne, W.K. Bischel, *J. Opt. Soc. Am. B* 15 (1998) 996.
- [10] N.V. Kuleshov, A.A. Lagatsky, A.V. Podlipensky, V.P. Mikhailov, *Opt. Lett.* 22 (1997) 1317.
- [11] N.V. Kuleshov, A.A. Lagatsky, V.G. Shcherbitsky, V.P. Mikhailov, E. Heumann, T. Jensen, A. Dening, G. Huber, *Appl. Phys. B* 64 (1997) 409.
- [12] M.C. Pujol, M. Rico, C. Zaldo, R. Solé, V. Nikolov, X. Solans, M. Aguiló, F. Díaz, *Appl. Phys. B* 68 (1999) 187.
- [13] R. Solé, V. Nikolov, X. Ruiz, J. Gavalda, X. Solans, M. Aguiló, F. Díaz, *J. Cryst. Growth* 169 (1996) 600.
- [14] M.C. Pujol, R. Solé, J. Gavalda, J. Massons, M. Aguiló, F. Díaz, *J. Mater. Res.* 14 (1999) 3739.
- [15] P.V. Klevtsov, L.P. Kozeeva, *Sov. Phys.-Dokl.* 14 (1969) 185.
- [16] L.I. Yudanov, A.A. Pavlyuk, O.G. Potapova, *Neorg. Mat.* 28 (1992) 2208.
- [17] D.E. McCumber, *Phys. Rev.* 136 (1964) 954.